REPORT DOCUMENTATION PAGE

Form Approved
OMB No. 0704-0188

AD-A233 119

2. Report Date.	3. Report Type and Dates Covered.
19910	Journal Article

Porosities, Permeabilities, and Microfabrics of Devonian Shales

5. Funding Numbers.

Program Element No.	61153N
Project No.	03205
Task No.	330
Accession No.	DN257003

6. Author(s).
David K. Davies, William R. Bryant, Richard K. Vessell, and Patti J. Burkett

7. Performing Organization Name(s) and Address(es).
Ocean Science Directorate
Naval Oceanographic and Atmospheric Research Laboratory
Stennis Space Center, MS 39529-5004

8. Performing Organization Report Number.
JA 360:007:90

9. Sponsoring/Monitoring Agency Name(s) and Address(es).
Ocean Science Directorate
Naval Oceanographic and Atmospheric Research Laboratory
Stennis Space Center, MS 39529-5004

10. Sponsoring/Monitoring Agency Report Number.
JA 360:007:90

11. Supplementary Notes.
MFS

12a. Distribution/Availability Statement.
Approved for public release; distribution is unlimited.

12b. Distribution Code.

13. Abstract *(Maximum 200 words)*.
Shales generally are regarded as source rocks and seals. However, in Illinois, Michigan, and Appalachian Basins, shales of Devonian age commonly are regarded as reservoir rocks. According to Broadhead et al. (1982), economic gas production from nonfractured shales has been an established fact in these basins for several decades. In some areas, natural fractures are an important control on production. In other areas, gas productive shale intervals lack natural fractures.

There is a general dearth of geological information and understanding regarding shales, particularly compared to that available on more conventional reservoir rocks (sandstones and carbonates). Shales are difficult to analyze because of their fine grain size, small pore size, and low values of porosity and permeability which approach the resolution levels of existing equipment. The pore structure and reservoir properties of shales are not well understood, despite their potential economic significance and importance in the geologic record.

This chapter reports on the structure of shale porosity, and documents relationships among porosity, permeability, and shale microfabric through combined analysis of geological and engineering data. It is part of an ongoing effort by the Gas Research Institute to understand and maximize Devonian shale production in the southern Appalachian Basin.

14. Subject Terms.	15. Number of Pages.
(U) Sediment Transport; (U) Pore Pressure; (U) Clay	12
	16. Price Code.

17. Security Classification of Report.	18. Security Classification of This Page.	19. Security Classification of Abstract.	20. Limitation of Abstract.
Unclassified	Unclassified	Unclassified	SAR

CHAPTER 10

Porosities, Permeabilities, and Microfabrics of Devonian Shales

David K. Davies, William R. Bryant, Richard K. Vessell, and Patti J. Burkett

Introduction

Shales generally are regarded as source rocks and seals. However, in the Illinois, Michigan, and Appalachian Basins, shales of Devonian age commonly are regarded as reservoir rocks. According to Broadhead et al. (1982), economic gas production from nonfractured shales has been an established fact in these basins for several decades. In some areas, natural fractures are an important control on production. In other areas, gas productive shale intervals lack natural fractures.

There is a general dearth of geological information and understanding regarding shales, particularly compared to that available on more conventional reservoir rocks (sandstones and carbonates). Shales are difficult to analyze because of their fine grain size, small pore size, and low values of porosity and permeability which approach the resolution levels of existing equipment. The pore structure and reservoir properties of shales are not well understood, despite their potential economic significance and importance in the geologic record.

This chapter reports on the structure of shale porosity, and documents relationships among porosity, permeability, and shale microfabric through combined analysis of geological and engineering data. It is part of an ongoing effort by the Gas Research Institute to understand and maximize Devonian shale production in the southern Appalachian Basin.

Data Base

The data base for this study consists of 118 drilled sidewall core samples from 17 wells in southeastern Ohio, eastern Kentucky, West Virginia, and Virginia (Fig. 10.1). Each sidewall core was drilled horizontally from the well bore, and is a small ($\approx 1 \times 3$ in.) conventional core. Core samples were analyzed to determine (1) petrographic characteristics (composition, texture, fabric, pore structure), (2) physical properties (porosity, permeability, saturation, and grain density), and (3) organic geochemistry (total organic carbon). Sample locations were not selected by the authors, but by engineers involved with log analysis and well stimulation. From a geological viewpoint, sample locations can be considered essentially random.

Prior to detailed analysis, each core was examined with a binocular microscope. Naturally fractured cores were not included in this study. Each core was cut into two portions, perpendicular to bedding. The first portion was used for geologic analysis and the second for physical properties analysis (Fig. 10.2). A complete set of analytical results is available in an open file report (Truman and Campbell, 1986).

Petrographic analyses involved routine thin section, X-ray diffraction (bulk and fine fraction) and scanning electron microscope (SEM) analysis of 118 core samples. Transmission electron microscope (TEM) analysis of ultrathin sections ($\approx$ 700 Å in thickness) was undertaken on 13 samples, using preparation techniques described by Bennett et al. (1977). These analyses were all carried out by the authors. Total organic carbon content (TOC) was determined by a commercial laboratory on 109 of the core samples.

Reservoir properties measurements used in this study include porosity (vol%), permeability (microdarcies, μd), and grain density (g/cm^3). The measurement of accurate values for these properties is difficult in low porosity rocks. A complete suite of results was unobtainable for some of the core samples due to small sample size, microfractures, and permeabilities below the minimum limits of detection (<0.001 μd). Results were obtained for the following numbers of cores: porosity, 113 samples; permeability, 68 samples; grain density, 113 samples.

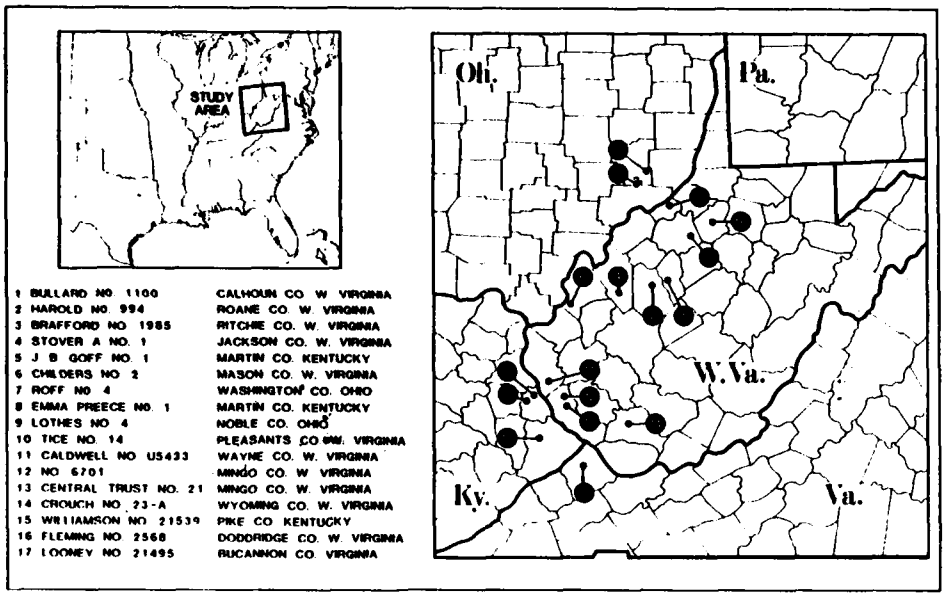

Figure 10.1. Location of study area and sampled wells.

Porosity was determined by subtraction of bulk volume from grain volume. Water was extracted from the cores using a Dean Stark extractor, after which samples were soxhlet cleaned with a chloroform–methanol mixture and dried in an oven at 40°C. Grain volume was measured in a Boyle's law apparatus with helium. No confining pressure was applied to the sample. Bulk volume was measured with calipers on cylindrical samples and by mercury immersion on irregular shapes.

Gas permeability was measured in a pulse-decay apparatus with nitrogen at a confining pressure of 2500 psi and a pore pressure of 1000 psi. This technique for the measurement of permeability is a transient system that minimizes the Klinkenberg gas-slippage effect. A small (25–50 psi) differential gas pressure is exerted across each core, and the change of gas pressure with time is recorded. Permeability is calculated from the rate of pressure decay with time (Walls, 1982; Walls et al., 1982). Bulk

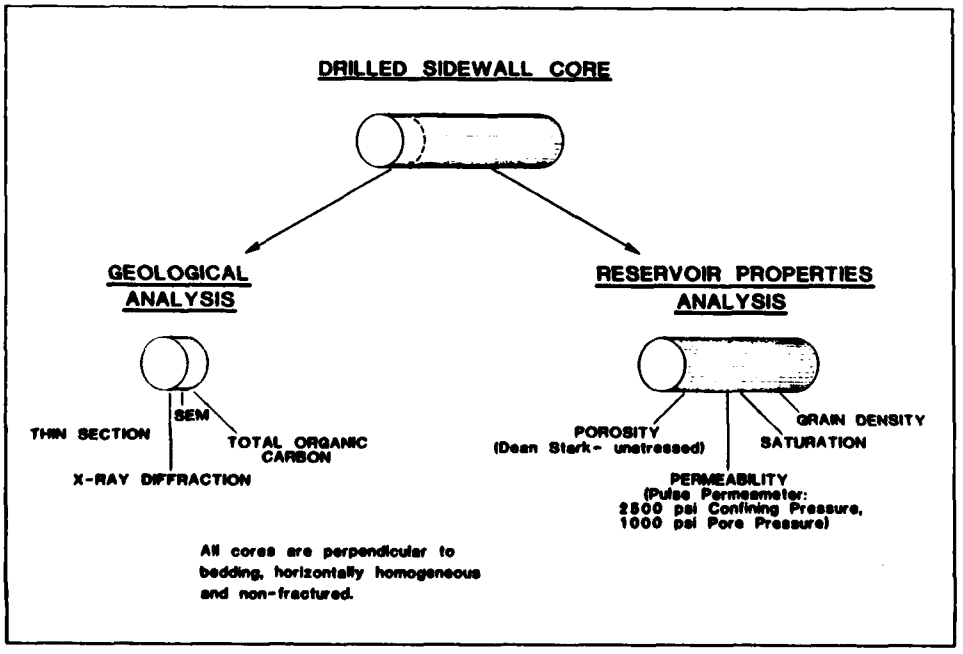

Figure 10.2. Analytical procedures attempted on all core samples.

Table 10.1. Microfabric and average mineralogy of each of the three types of Devonian Shale in the southern Appalachian Basin.*

Shale type	Shale fabric	Mineralogy (wt %)						TOC (wt %)
		Quartz + feldspar	Clay†	Pyrite	Siderite	Calcite	Dolomite†	
A	Chaotic–burrowed	47	47	3	1	1	1	0.5
B	Chaotic–subparallel	39	50	5	4	2	1	0.6
C	Parallel	48	45	6	Tr	Tr	Tr	4.7

*Based on SEM, X-ray diffraction, thin section, and organic geochemical analysis.
†Clay includes mica; dolomite includes ankerite.

density was calculated as preserved weight divided by bulk volume. All reservoir property measurements were performed by a commercial laboratory that specializes in the analysis of core samples with low values for porosity and permeability.

Devonian Shale Lithologies

The Devonian Shale sequence in the southern Appalachians averages some 3000 ft (1000 m) in thickness. This sequence consists dominantly of shales with occasional, thin, interbedded sandstones and siltstones. In this chapter the term "shale" is used for all rocks finer than sand grade that contain more than 35% clay and mica (Krynine, 1948, p. 154–155). Devonian shales are indurated and may or may not have fissility.

The average Devonian shale sample analyzed in this study contains approximately 45% detrital clay (including fine grained mica). Highly crystalline illite is virtually the only clay mineral recorded in X-ray diffraction analysis. The groundmass of the shale consists of an intermixture of finely crystalline illite and muscovite. Angular grains of detrital quartz ($\approx$ 40%) and feldspar (<5%) are scattered irregularly throughout the groundmass of illite/muscovite. Quartz and feldspar grains are usually of silt or very fine sand-size grade.

Three types of shales may be recognized in the sequence. These we refer to as shale Types A, B, and C. Discrimination among shale types is based on a combination of microfabric, mineralogy, and color distinctions (Table 10.1). The three varieties of shale grade into one another. Shale Types A and C may be regarded as end-members in a continuum that grades through shale Type B.

Shale Type A (Fig. 10.3)

This shale type is characterized by chaotic microfabric, commonly the result of intense burrowing activity. Burrowing activity has resulted in disruption of the original depositional fabric, and the plate-like illite/muscovite components have random orientation. Scattered silt grains supported the disrupted fabric during burial compaction. Traces of the original, laminated, depositional fabric may still be seen where burrowing is not intense. These shales are gray in color, contain less than 1% organic carbon, and have a low abundance of reducing minerals, e.g., pyrite (Table 10.1). They are interpreted as being deposited under aerobic bottom conditions.

Shale Type B (Fig. 10.4)

These shales contain less quartz and more authigenic minerals characteristic of reducing conditions than shale Type A (Table 10.1). Authigenic pyrite, siderite, and calcite are ubiquitous, and can be abundant locally. For example, the siderite content of individual cores ranges up to 35% and the pyrite content ranges up to 14%. High concentrations of these minerals in the small cores probably reflect the presence of nodules rather than continuous beds. Shale Type B has the highest average grain density of all rocks analyzed from the Devonian Shale sequence (2.77 g/cm^3, Table 10.2). This is the result of the abundance of "heavy" authigenic sulfide and carbonate minerals. Minor quantities of kerogen occur in the shale.

The microfabric is generally indistinct to subparallel, owing to a tendency for a combination of chaotic and subparallel grain alignment. The general absence of burrows in these rocks suggests deposition in dysaerobic bottom conditions, that shales of Type B may be of deeper water origin than the silty shales of Type A.

Shale Type C (Fig. 10.5)

This shale variety is generally referred to as "black shale" in the Appalachian Basin. Shales of Type C are characterized by high

Table 10.2. Mean values of reservoir properties for individual shale types, Devonian shales, southern Appalachian Basin.

Shale type	Porosity (%)	Permeability (μd)	Grain density (g/cm^3)
A	3.7	3.7	2.75
B	3.6	1.7	2.77
C	4.1	0.9	2.63

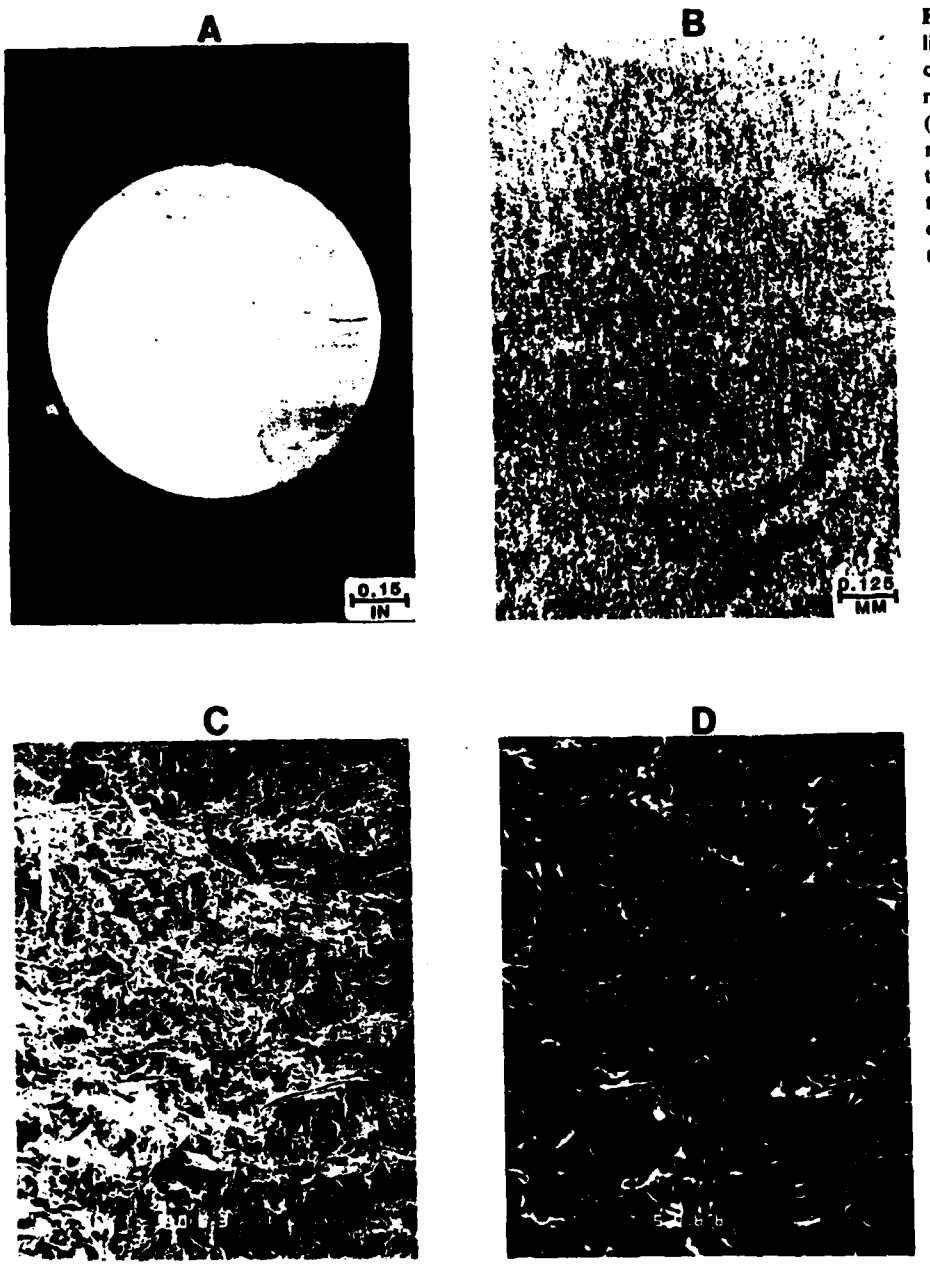

Figure 10.3. Photographs of shale Type A, illustrating lithology and microfabric. (A) View of the end of the core plug, cut perpendicular to bedding. Note the disruption of fabric due to burrowing (transmitted light). (B) Thin section view, at low magnification (plane polarized light). (C) Low magnification, SEM view shows the chaotic arrangement of detrital grains in this shale type. Scale = 100 μm. (D) Inverse polarity SEM view of the same area seen in C. Note the disorganization of the fabric elements (white).

values of TOC (Table 10.1). The total organic carbon content is always high, ranging from 1.24 to 21.35%. The organic material occurs as discrete kerogen fragments that can be large enough to be seen with the naked eye. Pyrite is also abundant and can compose up to 17% of the core samples in those intervals with pyrite nodules. Despite the pyrite content (grain density $\approx$ 4.99 g/cm^3), this rock type has the lowest grain density of all rocks analyzed. This reflects the presence of significant quantities of the low-density kerogen component (grain density $\approx$ 1.25 g/cm^3).

The shale fabric is dominated by abundant, well-defined, small-scale laminations. Small-scale parallel laminae are the result of grain segregation: silt-clay-rich laminae alternate with clay–organic-rich laminae. Laminations are frequently enhanced by plates of muscovite and elongate fragments of kerogen.

Black shales of the Devonian section are interpreted as the deepest water shales in the section. It is hypothesized that bottom conditions were anaerobic. This conclusion is supported by the absence of bioturbation and abundance of kerogen in these rocks. The anoxic bottom conditions inhibited life but were con-

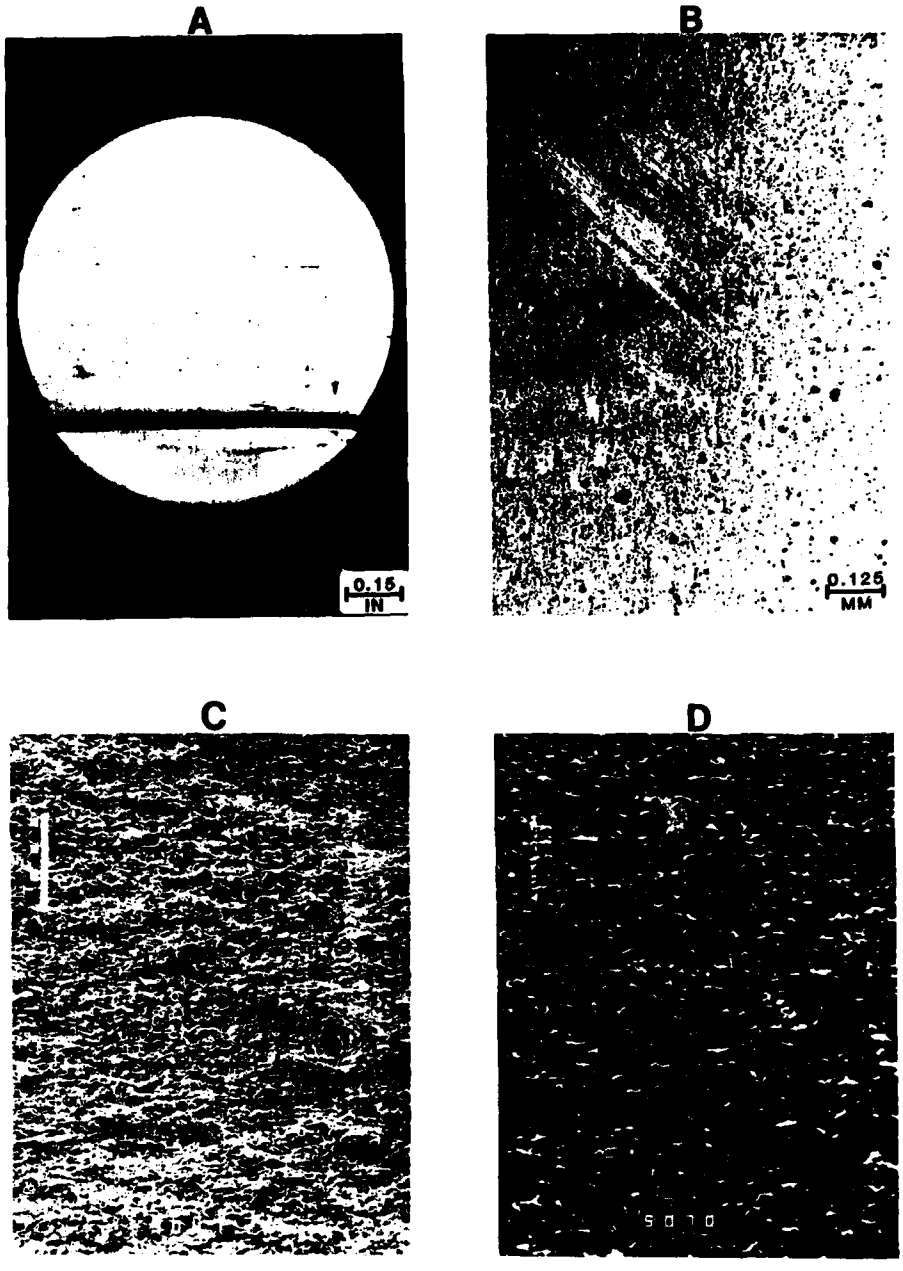

Figure 10.4. Photographs of shale Type B, illustrating lithology and microfabric. (A) View of the end of the core plug, cut perpendicular to bedding. Note the ill-defined microfabric. Plug was broken during thin sectioning, resulting in the horizontal fracture seen towards the base of the core end (transmitted light). (B) Thin section view, at low magnification. Black grains are authigenic pyrite (plane polarized light). (C) Low magnification, SEM view reveals that fabric elements have a greater degree of parallelism than in shale Type A. Scale = 100 μm. (D) Inverse polarity SEM view of the same area seen in C. Fabric elements (white) are generally short and have subparallel to parallel arrangement over much of the area in this view.

ducive to the preservation of lipid-rich, amorphous, and structured marine organic matter that would be destroyed under normal oxidizing conditions. The abundant pyrite resulted from the action of sulfide-reducing bacteria that flourished under these reducing conditions.

Porosity, Permeability, and Microfabric

The results of laboratory analysis of porosity and permeability are summarized in Table 10.2. Mean porosity values for each shale type range from 3.6 to 4.1% (Table 10.2). The highest porosity value and greatest range of porosity values (1.2–7.6%) occur in shale Type C. Evaluation of log-derived values of porosity also suggests that shale Type C contains streaks of relatively high porosity. For this reason, several operators in the study area preferentially perforate the black shales. The slightly higher values of porosity may indicate streaks of better sorting in these distal, deep water, Type C shales.

Mean values for permeability are strongly controlled by shale type (Table 10.2). These differences are not considered to be the result of mineralogical or lithological variations. There are no

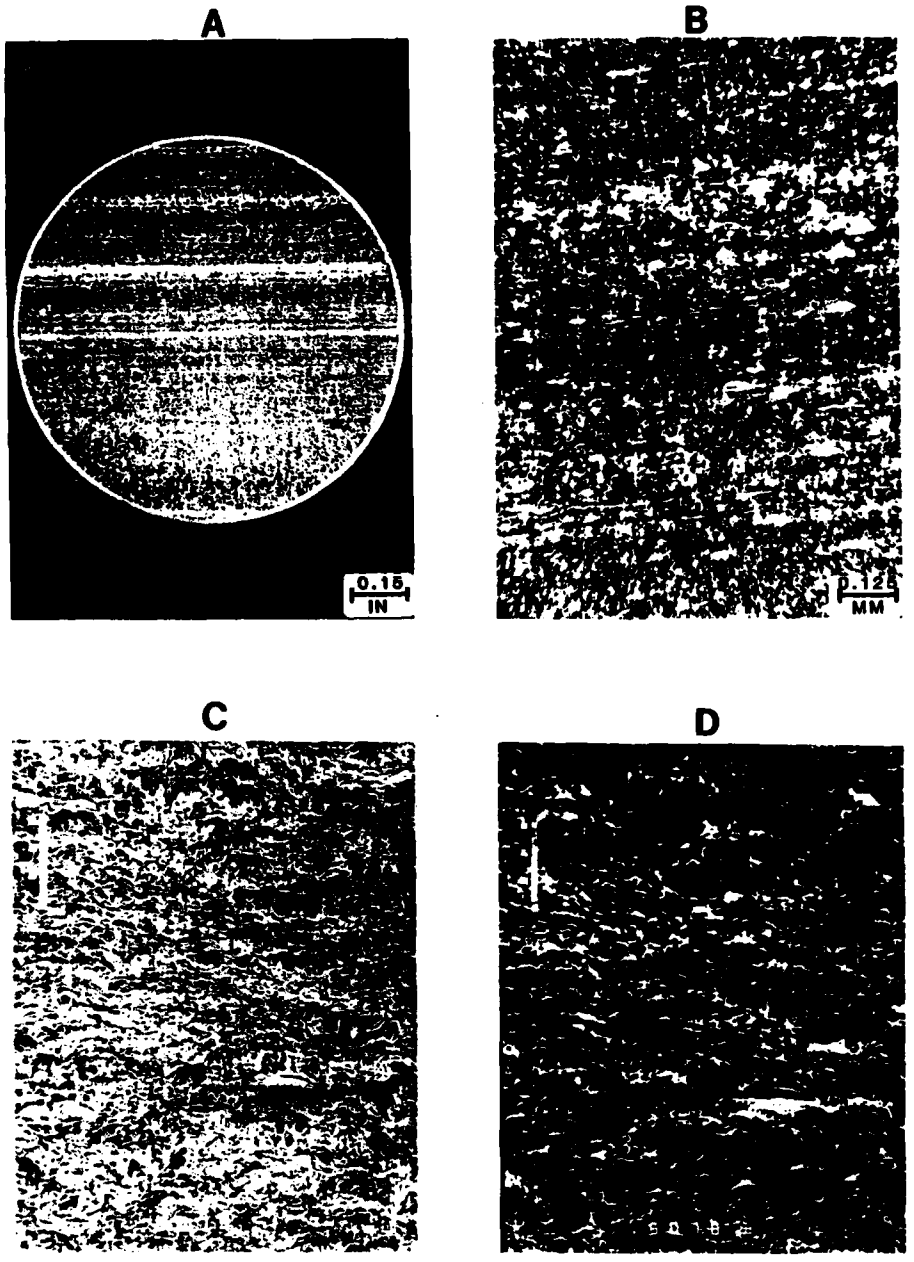

Figure 10.5. Photographs of shale Type C, illustrating lithology and microfabric. (A) View of the end of the core plug, cut perpendicular to bedding. Note the well laminated microfabric (transmitted light). (B) Thin section view, at low magnification. Lamination is well defined through segregation of quartz- and shale-rich laminae (plane polarized light). (C) Low magnification, SEM view reveals that fabric elements are well ordered and parallel. Scale = 100 μm. (D) Inverse polarity SEM view of the same area seen in C. Fabric elements (white) are longer more closely spaced and better defined than in shale Type B.

differences in the clay mineralogy or in the ratio of grains to matrix that would explain the observed permeability differences. In our opinion, microfabric is the fundamental control on shale permeability. Shale Type A, with random microfabric, has the highest permeability. Shale Type C, with laminated microfabric, has the lowest permeability. Shale Type B, with a fabric intermediate between shale Types A and C, has intermediate permeability. These results indicate that, for a given porosity, the permeability will be lowest in shales with laminated microfabric (black shales of Type C) and highest in shales with chaotic fabric (gray shales of Type A).

The fundamental controls on the fabric of Devonian shales appear to be factors present in the depositional environment. Shallow water shales, which have chaotic fabric, have been subjected to burrowing. Deep water shales, which are strongly laminated, show the absence of penecontemporaneous burrowing and retain their presumed, original depositional fabric. Similar environmental controls on shale fabric have been reported by O'Brien et al. (1980) and O'Brien (1987).

Relationships documented here between fabric and measured permeability have previously been recognized only qualitatively. In his work on Devonian shales, Soedder (1988, p. 122) noted

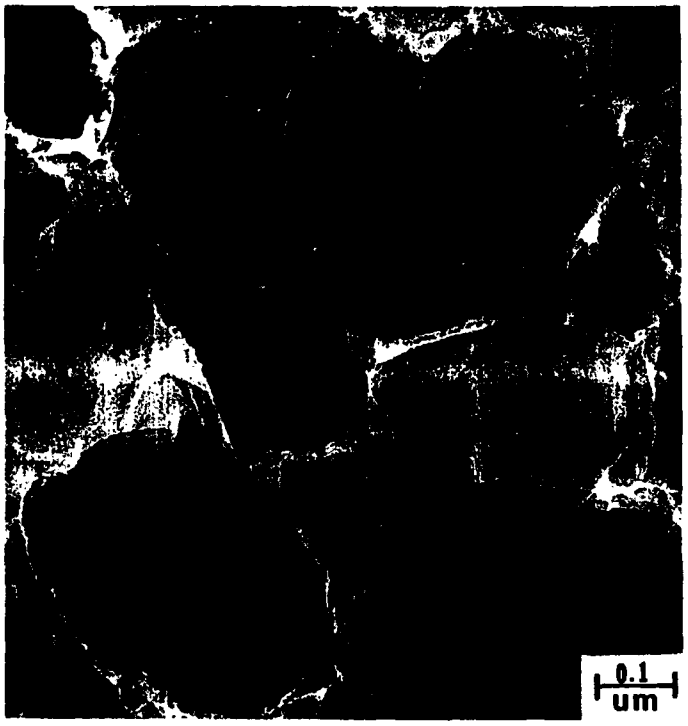

Figure 10.6. TEM photomicrograph of well-sorted, very fine-grained shale. Note the overlapping arrangement of detrital particles (gray/black) and intergranular pores (white). In all TEM views, black, opaque grains are ≈ 700 Å thick (the thickness of the ultrathin section). The thinner the particle, the lighter the gray shade. Random particle stacking produces alternating grains and pores within the 700 Å A plane of the section. White areas represent pores that extend completely through the section.

Figure 10.7. TEM photomicrograph of poorly sorted shale. Individual grains are illite and have disparate sizes and shapes. Intergranular pores (white) are common.

that "Differences between the depositional environment. . . had an influence on the pore geometry and microstructure of the resultant lithified shale. . . The presence or absence of oriented clay flakes would appear to have consequence with respect to pore size and connectivity in shales and requires further investigation."

Shale Texture and Pore Structure

Visual analysis of shale grain size, sorting, and pore structure was undertaken using ultrathin sections (thickness ≈ 700 Å) in a transmission electron microscope. Preparation difficulties restricted our views of shale pore systems to views that are generally parallel to the basal plane of the clay and mica components.

Detrital components in Devonian shales of all types range from well to poorly sorted (Figs. 10.6 and 10.7). Most are poorly sorted. Thin, plate-like flakes of detrital illite and mica overlap in random fashion. Several different flakes can overlap in the 700 Å thickness of the ultrathin section, indicating that the thinnest individual detrital clay particles have a thickness of 200–300 Å. Grain size is variable from sample to sample, the finest measured grain size of any sample in the data set being 0.2 μm. Visual porosity is of intergranular origin.

The poorly sorted shales are considerably more abundant than the well-sorted shales. Grain size is highly variable and difficult to measure in TEM because of the small size of the sample used in analysis. In the poorly sorted shales, large (sand and silt-sized) mica flakes, kerogens, and detrital quartz grains are surrounded by smaller flakes of illite that have widely varying sizes. It is not yet possible to section the quartz grains, thus results of TEM analysis in this chapter are selective for the illite-rich, finer grained portions of the rock. Figure 10.7 displays the general textural characteristics of the clay-rich portions of a poorly sorted shale. Most grains have irregular shape. Intergranular porosity is common: modal pore diameters range between 1 and 2 μm.

Image analysis of TEM negatives demonstrates the widespread distribution of porosity around the edges of detrital particles (Fig. 10.8). The pore system in the shales appears to be almost exclusively intergranular. The shape and size of the pores are variable, a function of the irregular size and shape of the surrounding grains. There is a relationship between the size of the detrital particles in the shales and the size of the associated

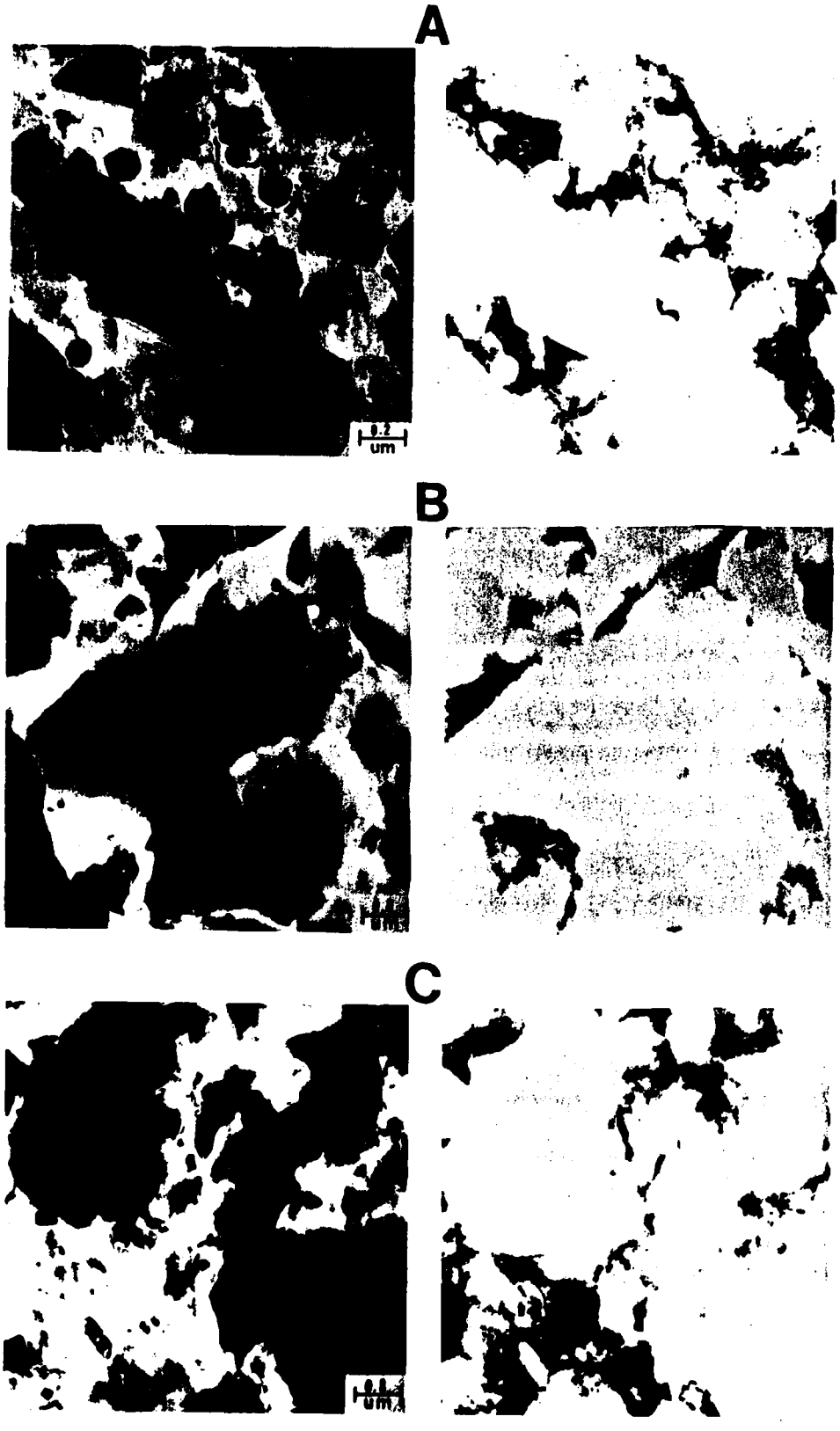

Figure 10.8. TEM photomicrographs (left) and matching, computer-generated images showing grains and pores (right). Porosity is white in the TEM photomicrographs and black in the matching images. (A) This sample has well-developed intergranular porosity. Octohedrons of authigenic pyrite (black) occur within the intergranular pore system. (B, C) These samples have porosity but lack authigenic pyrite. (Computer images are generated using quantitative values for gray shades taken from TEM negatives. These values are used to define grain and pore outlines.)

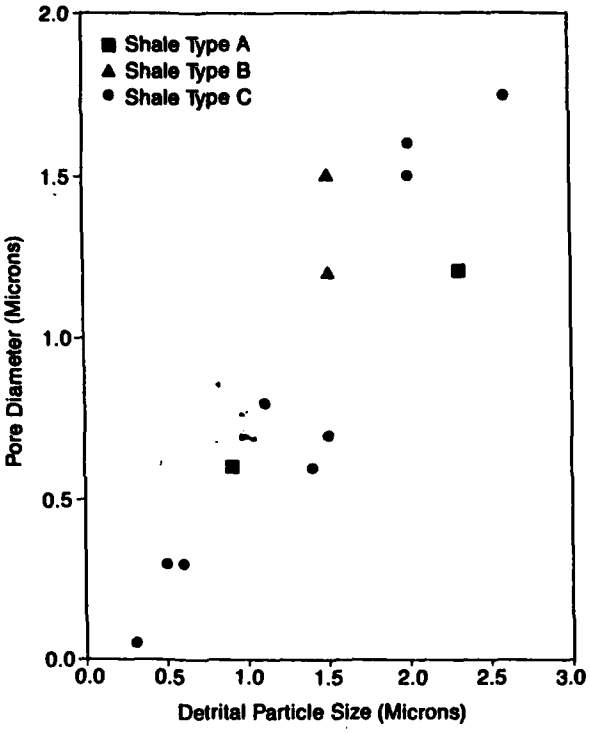

Figure 10.9. Cross-plot illustrating the relationship between particle size and pore diameter. Measurements were made using TEM images. Each data point represents a different image.

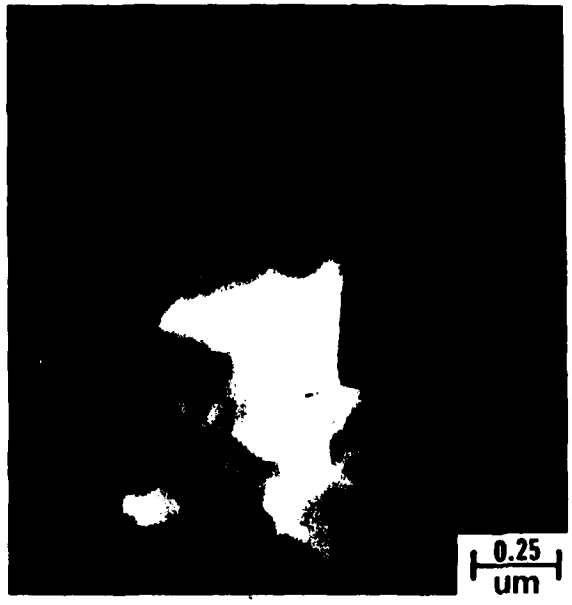

Figure 10.10. TEM photomicrograph of an intergranular pore (white) that is surrounded by illite flakes. Note that the illites are characterized by straight edges, interpreted as diagenetically developed crystal faces. (Photograph is slightly fuzzy due to high magnification.)

pores: the largest pores occur with the largest particles (Fig. 10.9). (This is the standard relationship that exists in sandstone pore systems of intergranular origin.) The relationship becomes increasingly diffuse as the sizes of grains and pores increase (Fig. 10.9).

High magnification views of pores reveal straight edges on illite flakes that may represent crystal faces (Fig. 10.10). The highly crystalline state of the illite indicates considerable diagenetic alteration. Diagenesis has also resulted in the precipitation of authigenic mineral phases in the intergranular shale pores (Figs. 10.8A and 10.11A). Pyrite octohedra are the most common of the authigenic, pore lining minerals. Unidentified, tabular minerals also occur. These may be apatite or a variety of zeolite. The authigenic minerals commonly occur along the pore walls (Fig. 10.11A). Three-dimensional reconstruction of a typical 2 μm pore (Fig. 10.11B) demonstrates that (1) the pores have irregular surfaces, (2) pore height increases away from the grain edges, and (3) 2-μm-long shale pores have a vertical dimension greater than the 700 Å thickness of the thin section.

Permeability and Porosity Considerations

Permeability values for Devonian shales in this study range from 10 to 10^{-2} μd (mean ≈ 2 μd). Permeability values are controlled strongly by microfabric. Shales with parallel microfabric consistently have lower permeabilities (<1 μd) than shales with chaotic microfabric (>1 μd). The commercial measurement techniques used in these analyses are considered state of the art (Walls, 1982; Walls et al., 1982). The absolute values reported here are at variance, however, with theoretical considerations and with evidence derived from direct observation of the shale pore system.

Laboratory experiments in consolidated muds and clays with porosity values of 10–20% yield permeabilities on the order of 10^{-5} μd. These values for permeability are several orders of magnitude lower than the values derived for this study using pulse permeametry.

Even if the absolute values for permeability reported here for Devonian shales are too high, there exists a consistent relationship between permeability and microfabric. Shales with chaotic fabric have higher permeability than shales with laminated microfabric. This relationship between permeability and fabric is supported by independent evidence. Soedder (1988, p. 123) pointed out that "Most gas shows occur in gray shales (Shale Types A and B)... not in the black units (Shale Type C)...At least some of the gray shale is fairly permeable to gas and may have been overlooked as a productive formation."

The porosity of Devonian shale samples, as measured by Dean Stark analysis, ranges from 1 to 8% (mean ≈ 4%). Values for porosity are less affected by changes in shale microfabric than are values for permeability. TEM observations of Devonian shale pore systems reveal that the pores are larger and more

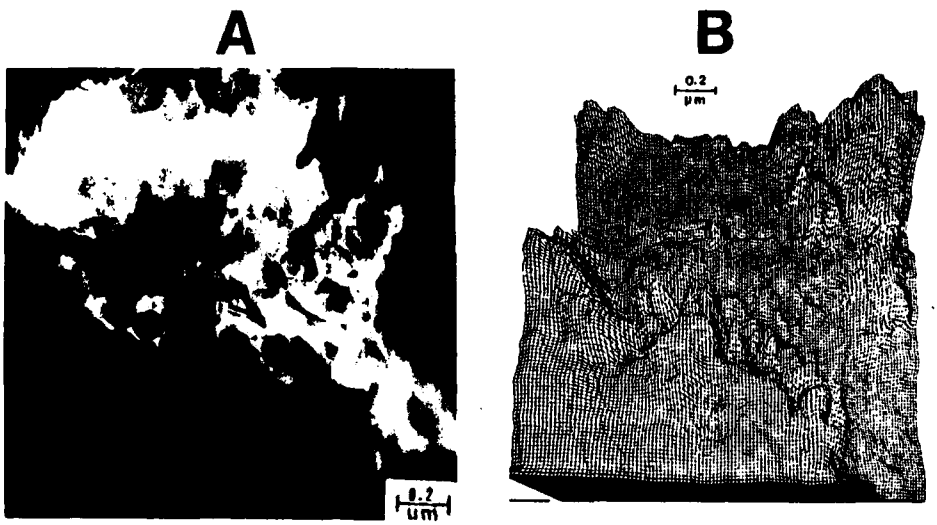

Figure 10.11. (A) TEM view of a single pore (maximum dimensions ≈ 2 µm × 1 µm × 700 Å. (A) The lower edge of this pore is lined with pyrite octohedra. The pore increases in depth away from the edges of the detrital grains. (B) Three-dimensional reconstruction of the pore seen in A, based on image processing of gray levels in the TEM negative.

abundant than would be anticipated from the results of commercial porosity analyses. Image analysis of TEM micrographs indicates that Devonian shales have values for TEM-derived porosity (optical porosity) that are higher than values derived from Dean Stark analysis. Most values for optical porosity average 7–8%. However, the TEM sample size is small (13 samples) and these results should be treated with caution.

Additional, indirect evidence for "true" shale porosity is available using production data derived from Devonian Shale gas wells. These wells almost always overproduce their estimated gas reserves, which are calculated on the basis of core- or log-derived porosity values. This is sometimes ascribed to adsorption of gas in kerogens. Alternately, or perhaps additionally, overproduction could be the result of the use of overly pessimistic values for porosity in the calculation of reserves.

Porosity values derived from TEM and Dean Stark analysis are considerably lower than would be anticipated from compaction experiments and theory. However, both sets of values for Devonian shales generally agree with values derived from ancient (Tertiary and Paleozoic) basins in Japan and Oklahoma (Athy, 1930; Hosoi, 1963). This suggests that geological age is an important control on the ultimate porosity of shales. Magara (1978, p. 31) stated, "This idea . . . contradicts Terzaghi's basic concept on stress balance among total stress, effective stress and fluid pressure." Magara (1978) further pointed out that Terzaghi's concept does not take into account possible effects on porosity that result from shale diagenesis.

TEM observations of shale pore systems in this study revealed that diagenetic modification is common. Pore space reduction has occurred as a result of (1) the precipitation of new mineral phases (Figs. 10.8A and 10.11A) and (2) possible increase in the size of detrital grains due to clay recrystallization (Fig. 10.10). Such changes require time and will reduce porosity.

What of the effects of diagenesis on basic particle orientation? Results presented here suggest that the Devonian shale retained much of the general characteristics of the original depositional fabric during burial diagenesis. Compaction obviously has reduced grain-to-grain spacing but does not appear to have influenced significantly the relative orientation of the individual particles. Shales deposited with random fabric during the Devonian still retain random fabric despite the influence of burial compaction. The growth of siderite, pyrite, and calcite concretions can be expected to alter original grain-to-grain relationships when such growth is displacive. This, however, is a relatively small scale, localized phenomenon, of minor importance when compared with the overall thickness of the Devonian Shale interval.

Comparison of the results of commercial laboratory analysis with the results of direct observation and theoretical considerations suggests that either (1) a large number of shale pores are not interconnected or (2) problems exist in current state-of-the-art commercial measurement techniques, particularly the measurement of permeability. Lack of connectivity of pores would result in Dean Stark porosity values that underestimate true porosity. This would explain the observed differences in porosity values. However, this explanation is inconsistent when applied to the results of the permeability analyses. Low values for measured porosity should be accompanied by low values for permeability. The fact that they are not indicates that significant problems exist with regard to currently used measurement techniques.

Conclusions

1. Microfabric is the fundamental control on permeability in non-fractured shales. Chaotic microfabric has the highest permeability; laminated microfabric has the lowest permeability.
2. At the range of magnification provided by the TEM, pores are dominantly intergranular in the Devonian shales of the study area.

3. Shale pores contain authigenic minerals, commonly pyrite.
4. Shale permeability may be influenced by the composition of the dominant clay mineral that controls grain shape and grain-to-grain relationships.
5. Experimental data suggest that permeability values derived from pulse permeametry may be too high and porosity values from Dean Stark analysis may be too low. This apparent discrepancy is a strong argument in favor of the necessity for changing or improving significantly on existing procedures for the measurement of porosity and permeability in tight, fine-grained rocks.

Acknowledgments

This project was funded principally by the Gas Research Institute, Contract Number 5086-213-1390, Dr. Richard Schepper, project director. Additional support was received from Texas A&M University, Department of Oceanography, and the Office of Naval Research.

References

Athy, L.F., 1930. Density, porosity and compaction of sedimentary rocks. Bulletin of the American Association of Petroleum Geologists, v. 14, p. 1-24.

Bennett, R.H., W.R. Bryant, and G.H. Keller, 1977. Clay fabric and geotechnical properties of selected submarine sediment cores from the Mississippi Delta. U.S. Dept. of Commerce, NOAA Professional Paper No. 9, 86 p.

Broadhead, R.F., R.C. Kepferle, and P.E. Potter, 1982. Stratigraphic and sedimentologic controls of gas in shale—example from upper Devonian of northern Ohio. Bulletin of the American Association of Petroleum Geologists, v. 66, p. 10-27.

Hosoi, H., 1963. First migration of petroleum in Akita and Yamagata Prefectures. Journal of Japanese Association of Mineralogists, Petrologists, and Economic Geologists, v. 49, p. 43-55, 101-114.

Krynine, P.D., 1948. The megascopic study and field classification of sedimentary rocks. Journal of Geology, v. 56, p. 130-165.

Magara, K., 1978. Compaction and fluid migration: practical petroleum geology. Developments in Petroleum Science. Elsevier, New York, 319 p.

O'Brien, N.R., 1987. The effects of bioturbation on the fabric of shale. Journal of Sedimentary Petrology, v. 57, p. 449-455.

O'Brien, N.R., K. Nakazawa, and S. Tokuhashi, 1980. Use of clay fabric to distinguish turbiditic and hemipelagic siltstones and silts. Sedimentology, v. 27, p. 47-61.

Soedder, D.J., 1988. Porosity and permeability of eastern Devonian gas shale. SPE Formation Evaluation, v. 3, p. 116-138.

Truman, R.B., and R.L. Campbell, 1986. Devonian shale well log interpretation. *Quarterly Report of the Gas Research Institute, Contract No.* 5085-213-1148 (unpubl.), 29 p.

Walls, J.D., 1982. Measurement of fluid salinity effects on tight gas sands with a computer controlled permeameter. SPE Paper 11092, 57th Annual Technical Conference Proceedings, New Orleans, Louisiana, p. 1-7.

Walls, J.D., A.M. Nur, and T. Bourbie, 1982. Effects of pressure and partial water saturation on gas permeability in tight sands: experimental results. SPE Journal Petroleum Technology, v. 34, p. 930-936.

Reprinted from

Richard H. Bennett, William R. Bryant, and Matthew H. Hulbert
Editors

Microstructure of Fine-Grained Sediments

Springer-Verlag
New York Berlin Heidelberg London
Paris Tokyo Hong Kong Barcelona